ЖЭТФ, 2016, том 149, вып. 1, стр. 121–130

NOETHER SYMMETRIES IN $f(G)$ GRAVITY

M. Sharif [a*], ***H. Ismat Fatima*** [a,b**]

[a] *Department of Mathematics, University of the Punjab Lahore-54590, Pakistan*

[b] *Department of Mathematics, Queen Mary College Lahore-54000, Pakistan*

Received June 24, 2015

We explore Noether symmetries of the Friedmann–Robertson–Walker universe model in modified Gauss–Bonnet gravity for both vacuum and nonvacuum (dust fluid) cases. We evaluate symmetry generators and the corresponding conserved quantities by using separation of variables and a power-law form. We construct exact $f(G)$ models and study accelerating expansion of the universe in terms of a scale factor, deceleration, and the EoS parameters. We also check the validity of energy conditions through the weak energy conditions for our constructed model. The state finder parameters indicate the resemblance of our constructed models to the ΛCDM model. We conclude that our results are consistent with the recent astrophysical observations.

DOI: 10.7868/S0044451016010107

1. INTRODUCTION

Recent observational evidence (like type-Ia supernovae, cosmic microwave background radiation, and large-scale structures) indicate that the universe is experiencing expansion at an accelerating rate, which has now become the central attraction of modern cosmology. In the scenario of general relativity (GR), a fluid with highly negative pressure is considered as a strong candidate to explain this phenomenon of the universe. This mysterious fluid with hidden features is termed dark energy (DE). The cosmological constant is the simplest DE model with the equation of state (EoS) parameter $\omega = -1$. But issues like fine-tuning and cosmic coincidence of this constant [1,2] motivated various dynamical models such as the quintessence, k-essence, and Chaplygin gas [3–5]. These models are obtained by modifying the matter part of the GR action, for which EoS parameter can move up and below the phantom dividing line $\omega = -1$.

Another approach to explaining the cosmic accelerated expansion is obtained by modifying the geometrical part of the action, resulting in modified theories like $f(R)$ gravity, Gauss–Bonnet gravity, modified Gauss–Bonnet gravity, etc. The modified Gauss–Bonnet theory of gravity ($f(G)$ theory) is obtained by adding an arbitrary function of G to the Einstein–Hilbert action [6]. The motivation of this modification comes from string theory via a low-energy effective scale [7]. This theory has been analyzed for cosmic expansion of the universe [8], from the standpoint of avoiding four types of finite-time future singularities [9, 10], with regard to solar system tests [11], thermodynamics [12–14], energy conditions [15, 16], and many other phenomena.

Energy conditions are used as basic ingredients to discuss various important phenomena like Hawking–Penrose singularity theorems, validity of the second law of black hole thermodynamics, and the positivity of energy density. These conditions arise from a the relation of the expansion scalar and the Raychaudhuri equation. Using the condition of the attractive nature of gravity for any hypersurface of orthogonal congruences (that rotation associated with the congruence defined by a null vector is zero) in these equations yields $R_{\mu\nu}v^\mu v^\nu \geq 0$ and $R_{\mu\nu}k^\mu k^\nu \geq 0$ for null (v^μ) and timelike (k^μ) vectors ($R_{\mu\nu}$ is the Ricci tensor). Replacing the Ricci tensor by the energy-momentum tensor in these inequalities, we obtain energy conditions. These are defined as the null energy condition ($\rho + p \geq 0$), the weak energy condition (WEC) ($\rho \geq 0$, $\rho+p \geq 0$), the strong energy condition (SEC) ($\rho+p \geq 0$, $\rho+3p \geq 0$), and the dominant energy condition ($\rho \geq 0$, $\rho \pm p \geq 0$). These conditions are completely geometri-

* E-mail: msharif.math@pu.edu.pk
** E-mail: ismatfatima4@gmail.com

cal statements and can be used for any theory of gravity [17].

Symmetry is a point transformation that maps solutions into solutions or leaves an object invariant. It helps us to find solutions of nonlinear differential equations by reducing them to linear ones. The main motivation comes from numerous conservation laws (energy, momentum, angular momentum, etc.) that are consequences of the presence of some kind of symmetry in a system. These conservation laws are special cases of the well-known Noether theorem, which provides a relation between symmetries of a physical system and conserved quantities. It states that if the Lagrangian of a physical system remains invariant under coordinate transformations, there is a corresponding conservation law.

Symmetries can be divided into Noether and Noether gauge symmetries (the latter are generalizations of Noether symmetries with the addition of a gauge term). The second type of symmetry provides some extra symmetry generators due to the existence of the gauge term. Noether symmetries have many significant applications in cosmology and theoretical physics and were introduced to find exact solutions of field equations [18, 19]. They have also been studied in modified theories such as the $f(R)$, $f(T)$ [20, 21], and scalar–tensor theories of gravity [22]. These theories have field equations with higher-order derivatives, and it is therefore difficult to find exact solutions in full generality without imposing particular a priori conditions. For this purpose, we use the Noether symmetry approach, which allows finding a closed system of equations, and we do not need to impose a particular function, which is instead selected by the Noether symmetry itself.

In [23], Noether symmetry was used to investigate universe evolution of the Friedmann–Robertson–Walker (FRW) model with scalar and vector fields in GR. These symmetries for a stringy charged black hole were explored in [24]. In [25], this approach was used to discuss stability of $f(R)$ models using FRW and spherically symmetric spacetimes in both vacuum and nonvacuum cases. In Palatini $f(R)$ gravity in the flat FRW model, $f(R)$ models and the exact cosmic scale factor were obtained in [26] using Noether symmetries. Some specific models of $f(R, G)$ gravity were discussed in [27] using the Noether symmetry approach. In [28], the coupling function and scalar field potential were explored using Noether and Noether gauge symmetry approaches in a modified scalar–tensor gravity. Solutions in the vacuum and nonvacuum cases were discussed for locally rotationally symmetric (LRS) Bianchi I (BI) geometry. Recently, exact solutions in $f(R)$ gravity for the BI model were found via Noether symmetry [29]. A linear scalar field and a constant potential were found in [30] using Noether gauge symmetry in the Gauss–Bonnet dilatonic theory of gravity.

In this paper, we construct some interesting $f(G)$ models in the background of the FRW universe model using the Noether symmetry approach. The plan of the paper is as follows. In the next section, we briefly review Noether symmetry and $f(G)$ gravity. Section 3 is devoted to a discussion of Noether symmetry generators in both vacuum and nonvacuum cases using separation of variables and a power-law form. We also evaluate conserved quantities, energy conditions, cosmological deceleration, and EoS parameters as well as state finder parameters. Finally, Section 4 concludes the results.

2. NOETHER SYMMETRY AND $f(G)$ GRAVITY

In this section, we briefly review Noether symmetry and the $f(G)$ theory of gravity. If the Lie derivative of a Lagrangian $\mathcal{L}$ with respect to a vector field X vanishes

$$L_X\mathcal{L} = 0, \tag{1}$$

then X is known as a Noether symmetry of the system. It relates many conservation laws to the symmetries of internal variables of a system, time, and space [31]. For point transformations (transformations of generalized coordinates q^i) that depend on an infinitesimal parameter ε, i. e., for $Q^i = Q^i(q^j, \varepsilon)$, we can introduce a vector field X of generalized coordinates as

$$X = \eta^i(q^j)\frac{\partial}{\partial q^i} + \left[\frac{d}{dt}(\eta^i(q^j))\right]\frac{\partial}{\partial \dot{q}^i}, \tag{2}$$

on the tangent space $TQ = \{q^i, \dot{q}^i\}$ related to the configuration space $Q = \{q^i\}$. Here, the dot denotes the time derivative, and η^i are unknown functions to be determined. Equation (2) represents a Noether symmetry if it satisfies Eq. (1). The Euler–Lagrange equations are

$$\frac{\partial\mathcal{L}}{\partial q^i} - \frac{d}{dt}\left(\frac{\partial\mathcal{L}}{\partial\dot{q}^i}\right) = 0, \tag{3}$$

and the associated energy function is

$$\mathbb{E} = \Sigma\dot{q}^i\frac{\partial\mathcal{L}}{\partial\dot{q}^i} - \mathcal{L}.$$

The conserved quantity is given by

$$\mathbb{I} = \eta^i\frac{\partial\mathcal{L}}{\partial\dot{q}^i}.$$

In Gauss–Bonnet gravity, the GR action comprises the Gauss–Bonnet invariant only, while in modified Gauss–Bonnet gravity, we replace G with an arbitrary function $f(G)$. The idea of $f(G)$ gravity is just like that of $f(R)$ gravity, and hence its action is given by [32]

$$S = \frac{1}{2\kappa^2}\int d^4x\sqrt{-g}\,[R + f(G)], \tag{4}$$

where $\kappa^2 = 8\pi\mathcal{G}$ is the coupling constant. Varying this action with respect to $g_{\mu\nu}$, we obtain the field equations

$$R_{\mu\nu} - \frac{1}{2}Rg_{\mu\nu} + 8\Big[R_{\mu\rho\nu\sigma} + R_{\rho\nu}g_{\sigma\mu} - R_{\rho\sigma}g_{\nu\mu} - \\ - R_{\mu\nu}g_{\sigma\rho} + R_{\mu\sigma}g_{\nu\rho} + \frac{1}{2}R(g_{\mu\nu}g_{\sigma\rho} - g_{\mu\sigma}g_{\nu\rho})\Big]\nabla^\rho\nabla^\sigma f_G + \\ + (Gf_G - f)g_{\mu\nu} = 0,$$

where the subscript G denotes the derivative of f with respect to G, while $R_{\mu\nu}$ and $R_{\mu\nu\sigma\rho}$ are the Ricci and Riemann tensors. The Gauss–Bonnet invariant is

$$G = R^2 - 4R_{\mu\nu}R^{\mu\nu} + R_{\mu\nu\sigma\rho}R^{\mu\nu\sigma\rho}.$$

3. SOME EXACT $f(G)$ MODELS AND COSMOLOGICAL PARAMETERS

In this section, we adopt the Noether symmetry approach to solve the field equations for the FRW metric by considering both vacuum and nonvacuum cases. The flat FRW universe model is given by

$$ds^2 = dt^2 - a^2(t)(dx^2 + dy^2 + dz^2),$$

where $a(t)$ measures the expansion scale of the universe and is called the scale factor. The corresponding Gauss–Bonnet invariant is

$$G = 24\frac{\dot{a}^2\ddot{a}}{a^3}.$$

3.1. Vacuum case

In this case, action (4) takes the form

$$S = \int dt\,\mathcal{L}(q^i, \dot{q}^i) = \int dt\,\mathcal{L}(a, \dot{a}, G, \dot{G}).$$

The Lagrange multiplier method can be used to solve this action by considering G as a dynamical constraint. By choosing a suitable Lagrange multiplier and integrating by parts, we eliminate higher-order derivatives to write the Lagrangian in the standard mathematical form. Thus,

$$S = \int dt\left[\sqrt{-g}f(G) - \Upsilon\left(G - 24\frac{\ddot{a}\dot{a}^2}{a^3}\right)\right], \tag{5}$$

where Υ is the Lagrange multiplier. Varying this action with respect to G, we obtain $\Upsilon = \sqrt{-g}f_G$, $\sqrt{-g} = a^3$, and hence Eq. (5) becomes

$$S = \int dt\sqrt{-g}\left[f(G) - f_G\left(G - 24\frac{\ddot{a}\dot{a}^2}{a^3}\right)\right].$$

Integrating by parts, we obtain the Lagrangian density

$$\mathcal{L} = -8\dot{a}^3\dot{G}f_{GG} + a^3[f(G) - Gf_G]. \tag{6}$$

Euler–Lagrange equations (3) lead to

$$16\frac{\dot{a}\ddot{a}}{a^3}\dot{G}f_G + 8\frac{\dot{a}^2}{a^2}\ddot{G}f_G + 8\frac{\dot{a}^2}{a^2}\dot{G}f_G = -f(G) + Gf_G, \tag{7}$$

$$-24\frac{\dot{a}^2\ddot{a}}{a^3}f_{GG} - 8\frac{\dot{a}^3}{a^3}\dot{f}_{GG} = -f_G, \tag{8}$$

and the corresponding energy function becomes

$$\mathbb{E} = 24\frac{\dot{a}^3}{a^3} - \frac{1}{\dot{G}f_{GG}}(f(G) - Gf_G). \tag{9}$$

The Gauss–Bonnet pressure p_G is found from Eq. (7) as

$$p_G = 16\frac{\dot{a}\ddot{a}}{a^3}\dot{G}f_G + 8\frac{\dot{a}^2}{a^2}\ddot{G}f_G + f(G) - Gf_G, \tag{10}$$

and the Gauss–Bonnet density ρ_G can be obtained using Eq. (9) as

$$\rho_G = 24\frac{\dot{a}^3}{a^3}\dot{G}f_{GG} - f(G) + Gf_G. \tag{11}$$

The corresponding EoS parameter $\omega_G = p_G/\rho_G$ takes the form

$$\omega_G = \frac{16\frac{\dot{a}\ddot{a}}{a^3}\dot{G}f_G + 8\frac{\dot{a}^2}{a^2}\ddot{G}f_G + f(G) - Gf_G}{24\frac{\dot{a}^3}{a^3}\dot{G}f_{GG} - f(G) + Gf_G}. \tag{12}$$

The existence of a Noether symmetry is guaranteed by the existence of vector field (2) for which at least one of the unknowns $\eta^i(q^j)$ is nonzero. In the present case, the vector field of the generator is defined as

$$X = \alpha\frac{\partial}{\partial a} + \beta\frac{\partial}{\partial G} + \dot{\alpha}\frac{\partial}{\partial\dot{a}} + \dot{\beta}\frac{\partial}{\partial\dot{G}}, \tag{13}$$

on the tangent space $TQ = \{a, G, \dot{a}, \dot{G}\}$ of the configuration space $Q = \{a, G\}$. Here, $\alpha = \alpha(a, G)$ and $\beta = \beta(a, G)$ are symmetry generators to be found and

$$\dot{\alpha} = \dot{a}\frac{\partial\alpha}{\partial a} + \dot{G}\frac{\partial\alpha}{\partial G}, \quad \dot{\beta} = \dot{a}\frac{\partial\beta}{\partial a} + \dot{G}\frac{\partial\beta}{\partial G}.$$

Equations (1) and (13) imply that

$$X\mathcal{L} = 0,$$

which leads to

$$3\alpha(f(G)-Gf_G)-\beta a f_G=0, \tag{14}$$

$$3\frac{\partial\alpha}{\partial a}f_{GG}+\frac{\partial\beta}{\partial G}f_{GG}=0, \tag{15}$$

$$\frac{\partial\alpha}{\partial G}f_{GG}=0, \tag{16}$$

$$\frac{\partial\beta}{\partial a}f_{GG}=0, \tag{17}$$

where α, β, $f(G)$, and $a(t)$ are unknowns to be determined. We solve this set of equations using the method of separation of variables and a power-law form.

3.1.1. Separation of variables

First, we solve Eqs. (14)–(17) by separation of variables. For this, we set

$$\alpha=A_1(a)A_2(G),\quad \beta=B_1(a)B_2(G), \tag{18}$$

where A_1, A_2, B_1, and B_2 are unknowns to be determined. Solving Eqs. (16) and (17) using Eq. (18), we obtain

$$\alpha=a_0A_1(a),\quad \beta=b_0B_2(G), \tag{19}$$

where a_0 and b_0 are arbitrary constants. From Eqs. (19) in (15), it follows that

$$\alpha=\lambda a(t)+a_0a_1,\quad \beta=-3\lambda G+b_0b_1, \tag{20}$$

where a_1 and b_1 are arbitrary constants and λ is the separation constant. It can be easily verified that Eq. (20) is consistent with Eqs. (15)–(17). Using Eq. (20) in (14), we obtain

$$f(G)=k\left(b_0b_1a(t)+3a_0a_1G\right)^{\lambda a(t)/a_0a_1+1}, \tag{21}$$

where k is the constant of integration. The symmetry generator takes the form

$$X=(\lambda a(t)+a_0a_1)\frac{\partial}{\partial a}+(b_0b_1-3\lambda G)\frac{\partial}{\partial G}.$$

The corresponding conserved quantity is given by

$$\mathbb{I}=\alpha\frac{\partial\mathcal{L}}{\partial\dot a}+\beta\frac{\partial\mathcal{L}}{\partial\dot G}=$$
$$=-8f_G(3\lambda a\dot a^2\dot G+3a_0a_1\dot a^2\dot G+b_0b_1\dot a^3-3\lambda\dot a^3G).$$

Using Eq. (21) in (8), we have

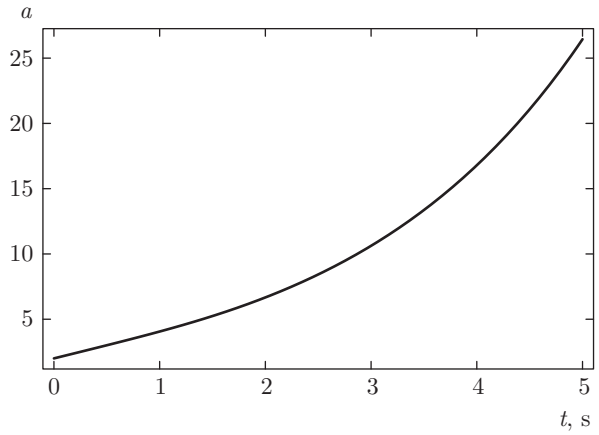

Fig. 1. Plot of the scale factor a versus time t

$$-72ka_0a_1\lambda a(t)\left(\frac{\lambda a(t)}{a_0a_1}+1\right)\times$$
$$\times\left(b_0b_1a(t)+3a_0a_1G\right)^{\lambda a(t)/a_0a_1-1}-24k\lambda a(t)\frac{\dot a^3}{a^3}\times$$
$$\times\dot G\left(\frac{\lambda a(t)}{a_0a_1}-1\right)\left(\frac{\lambda a(t)}{a_0a_1}+1\right)\times$$
$$\times\left(b_0b_1a(t)+3a_0a_1G\right)^{\lambda a(t)/a_0a_1-2})+$$
$$+ka_0a_1\left(\frac{\lambda a(t)}{a_0a_1}+1\right)\times$$
$$\times\left(b_0b_1a(t)+3a_0a_1G\right)^{\lambda a(t)/a_0a_1}=0. \tag{22}$$

We solve this equation numerically for the scale factor a by assigning the values $a_0=1$, $a_1=2$, $b_0=0.5$, $b_1=2$, $\lambda=3$ and $k=1$ with the initial conditions $a(0)=2$, $\dot a(0)=3$. The graphical behavior of the scale factor is shown in Fig. 1, indicating positively increasing behavior with the passage of time. Such a behavior shows expansion of the universe at an accelerating rate. We take the cosmological redshift $a(t)=a_0/(1+z)$ (where $a_0=1$ is the current value of the scale factor) for graphical representation of the EoS parameter shown in Fig. 2*a*, which represents negative increasing behavior with increasing the redshift z. This means that the universe is in the present DE era, $\omega_G<-1$ (phantom-fluid-dominated era) in the far future when the Gauss–Bonnet term is dominant. The deceleration parameter q is defined as

$$q=\frac{d}{dt}\left(\frac{1}{H}\right)-1.$$

The graphical behavior of q is shown in Fig. 2*b*. This indicates that q approaches zero as z takes large values and is negative for a late universe (the present and future eras) showing an accelerated phase of the expanding universe.

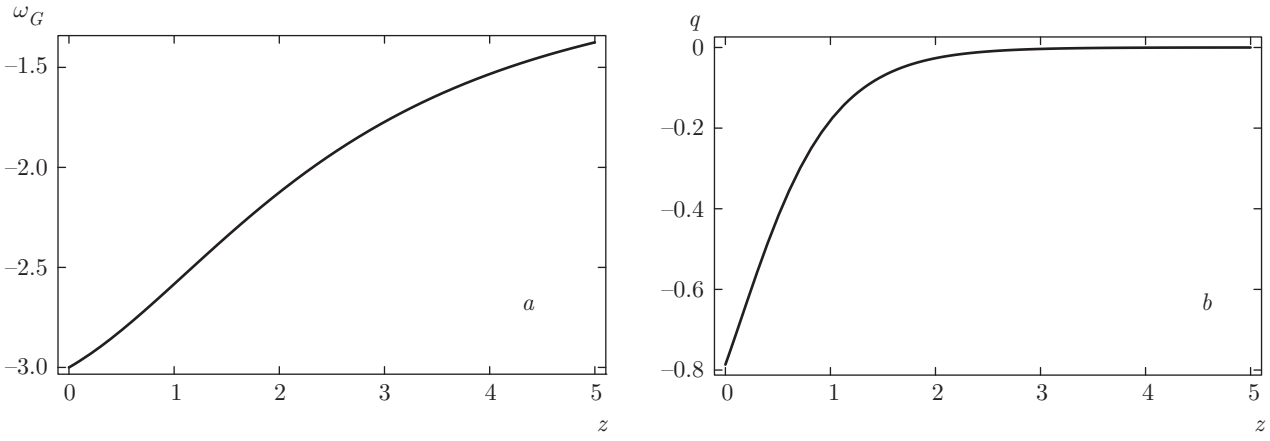

Fig. 2. The evolution of the EoS parameter ω_G (a) and the deceleration parameter q (b) versus the redshift z

3.1.2. Power-law form

Here, we use the power-law approach to solve the system of equations (14)–(17). For this, we take symmetry generators as

$$\alpha = \alpha_0 a^{\mu_0} G^{\mu_1}, \quad \beta = \beta_0 a^{\nu_0} G^{\nu_1}, \tag{23}$$

where the unknown powers μ_0, μ_1, ν_0, and ν_1 are to be determined. Equations (16) and (17) with Eq. (23) imply that $\mu_1 = \nu_0 = 0$, for which Eq. (23) becomes

$$\alpha = \alpha_0 a^{\mu_0}, \quad \beta = \beta_0 G^{\nu_1}. \tag{24}$$

Using these values in (15) with $\alpha_0 = \beta_0$ (without any loss of generality), we obtain $\nu_1 = 1$ and $\mu_0 = 1/3$, and hence

$$\alpha = \alpha_0 a^{1/3}, \quad \beta = \alpha_0 G. \tag{25}$$

The function $f(G)$ is obtained by using Eqs. (14) and (25) as

$$f(G) = k_1 G^{3/(a^{2/3}+3)}, \tag{26}$$

where k_1 is another constant of integration. The symmetry generators become

$$X = \alpha_0 a^{1/3} \frac{\partial}{\partial a} + \alpha_0 G \frac{\partial}{\partial G},$$

and the corresponding conserved quantity is

$$\mathbb{I} = -8\alpha_0 \dot{a}^2 (3a^{1/3}\dot{G} + \dot{a}G) f_{GG}.$$

Inserting $f(G)$ in Eq. (8), we obtain the scale factor

$$a(t) = c_1 e^{t^2/3} + c_2, \tag{27}$$

where c_1 and c_2 are constants of integration. Its graphical representation is shown in Fig. 3 with $c_1 = 2$ and

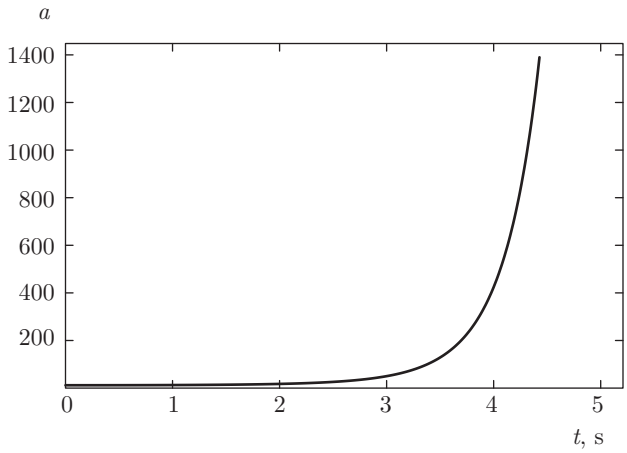

Fig. 3. Plot of the scale factor a versus t

$c_2 = 0$, which indicates the expanding nature of the universe at an accelerating rate due to its rapidly increasing behavior. Consequently, the function $f(G)$ becomes

$$\begin{gathered} f(G) = k_1 G^{3/(c_1^{2/3} e^{2t^2/9}+3)}, \\ G = \frac{32t^2}{27}\left(1+\frac{t^2}{3}\right). \end{gathered} \tag{28}$$

The deceleration parameter is given by

$$q = -\frac{2t^2 + e^{t^2/3}}{2t^2 e^{t^2/3}}.$$

In terms of the redshift z, the above equation takes the form

$$q = -\frac{6\ln\left|\dfrac{1}{c_1}\left(\dfrac{1}{z}+1\right)\right| + \dfrac{1}{c_1}\left(\dfrac{1}{z}+1\right)}{6\ln\left|\dfrac{1}{c_1}\left(\dfrac{1}{z}+1\right)\right| \dfrac{1}{c_1}\left(\dfrac{1}{z}+1\right)}. \tag{29}$$

Figure 4*a* shows that $q \to 0$ as $z \to \infty$ and $q \to -1$ for the present ($z = 0$) and future ($z < 0$) eras of the universe. This indicates the accelerating phases of the expanding universe from early to late time.

The EoS parameter takes the form

$$\omega_G = -\frac{k_1\left(\frac{5}{c_1e^{2t^2/9}+3}+1+\frac{32t^2}{c_1e^{2t^2/9}+3}\left[\frac{64}{9}t^2\left(\frac{2t^2}{3}+1\right)\right]^{-1}\right)}{\frac{c_1e^{2t^2/9}}{c_1e^{2t^2/9}+3}\left(k_1+\frac{64t^3}{c_1e^{2t^2/9}+3}\left[\frac{64}{9}t^2\left(\frac{2t^2}{9}+3\right)\right]^{-2c_1e^{2t^2/9}/(c_1e^{2t^2/9}+3)}\right)},$$

which in terms of redshift takes the form

$$\omega_G = -k_1\left[\frac{5}{\frac{1}{c_1}\left(\frac{1}{z}+1\right)^{2/3}+3}+1+\frac{96\ln\left|\frac{1}{c_1}\left(\frac{1}{z}+1\right)\right|}{\frac{1}{c_1}\left(\frac{1}{z}+1\right)^{2/3}+3}\left\{\frac{64}{3}\ln\left|\frac{1}{c_1}\left(\frac{1}{z}+1\right)\right|\left(2\ln\left|\frac{1}{c_1}\left(\frac{1}{z}+1\right)\right|+1\right)^{-1}\right\}\right]\times$$
$$\times\left[\frac{\frac{1}{c_1}\left(\frac{1}{z}+1\right)^{2/3}}{\frac{1}{c_1}\left(\frac{1}{z}+1\right)^{2/3}+3}\left\{k_1+\frac{64\left(3\ln\left|\frac{1}{c_1}\left(\frac{1}{z}+1\right)\right|\right)^{3/2}}{\frac{1}{c_1}\left(\frac{1}{z}+1\right)+3}\times\right.\right.$$
$$\left.\left.\times\frac{64}{3}\ln\left|\frac{1}{c_1}\left(\frac{1}{z}+1\right)\right|\left(2\ln\left|\frac{1}{c_1}\left(\frac{1}{z}+1\right)\right|+1\right)^{-2\frac{1}{c_1}\left(\frac{1}{z}+1\right)^{3/2}/\left(\frac{1}{c_1}\left(\frac{1}{z}+1\right)^{3/2}+3\right)}\right\}\right]^{-1}. \quad (30)$$

Its behavior is shown in Fig. 4*b* for $k_1 = 1$. This is negatively increasing behavior for large values of the redshift z, showing that the universe is in the present DE era, $\omega_G < -1$ (phantom-fluid-dominated era) in the far future.

The state finder parameters (r, s) are very useful to check the correspondence of the standard universe models with the constructed models. For example, $(r, s) = (1, 0)$ shows the correspondence of the constructed model with the ΛCDM model. These parameters are defined as

$$r = q + 2q^2 - \frac{\dot{q}}{H}, \quad s = \frac{r-1}{3(q-1/2)}.$$

In our case, these become

$$r = -\frac{2t^2+e^{t^2/3}}{2t^2e^{t^2/3}} + 2\left(\frac{2t^2+e^{t^2/3}}{2t^2e^{t^2/3}}\right)^2 - \frac{2t^4-3e^{t^2/3}}{9t^2e^{t^2/3}}, \quad (31)$$

$$s = \frac{r-1}{3\left(-\frac{2t^2+e^{t^2/3}}{2t^2e^{t^2/3}}\right)-\frac{1}{2}}. \quad (32)$$

These are shown in Fig. 5, which indicates that the curve passes through the point $(r, s) = (1, 0)$ representing the correspondence with ΛCDM model.

We now verify the energy conditions in this case. With Eqs. (10) and (11), these conditions in $f(G)$ gravity become

$$\text{NEC}: \rho_G + p_G \geq 0,$$
$$\text{WEC}: \rho_G \geq 0, \quad \rho_G + p_G \geq 0,$$
$$\text{SEC}: \rho_G + p_G \geq 0, \quad \rho_G + 3p_G \geq 0,$$
$$\text{DEC}: \rho_G \geq 0, \quad \rho_G \pm p_G \geq 0.$$

In the following analysis, we explore only the behavior of the WEC in exemplifying the application of energy conditions and the SEC for accelerated expansion of the universe. The expression for the WEC is

$$\mathrm{WEC} = \frac{c_1 e^{2t^2/9}}{c_1 e^{2t^2/9}+3}\left(k_1 + \frac{64t^3}{c_1 e^{2t^2/9}+3}\times \right.$$
$$\left. \times \left[\frac{64}{9}t^2\left(\frac{2t^2}{9}+3\right)\right]^{-2c_1 e^{2t^2/9}/(c_1 e^{2t^2/9}+3)}\right),$$

$$\frac{c_1 e^{2t^2/9}}{c_1 e^{2t^2/9}+3}\left(k_1 + \frac{64t^3}{c_1 e^{2t^2/9}+3}\times \right.$$
$$\left. \times \left[\frac{64}{9}t^2\left(\frac{2t^2}{9}+3\right)\right]^{-2c_1 e^{2t^2/9}/(c_1 e^{2t^2/9}+3)}\right) +$$
$$+ k_1\left(\frac{5}{c_1 e^{2t^2/9}+3}+1+\frac{32t^2}{c_1 e^{2t^2/9}+3}\times \right.$$
$$\left. \times \left[\frac{64}{9}t^2\left(\frac{2t^2}{3}+1\right)\right]^{-1}\right),$$

which is shown in Fig. 6 versus time t. We note that ρ_G initially increases positively for $t = 1$ s, then decreases until $t = 2.3$ s but remains positive, and finally it increases positively throughout the range of t. Figure 6*b* shows the plot of $\rho_G + p_G$, which represents decreasing but positive behavior with respect to t. Consequently, the WEC is satisfied for all values of t. For the behavior of the SEC ($\rho_G + 3p_G$), we find its expression

$$\mathrm{SEC} = \frac{c_1 e^{2t^2/9}}{c_1 e^{2t^2/9}+3}\left(k_1 + \frac{64t^3}{c_1 e^{2t^2/9}+3}\times \right.$$
$$\left. \times \left[\frac{64}{9}t^2\left(\frac{2t^2}{9}+3\right)\right]^{-2c_1 e^{2t^2/9}/(c_1 e^{2t^2/9}+3)}\right) +$$
$$+ 3k_1\left(\frac{5}{c_1 e^{2t^2/9}+3}+1+\frac{32t^2}{c_1 e^{2t^2/9}+3}\times \right.$$
$$\left. \times \left[\frac{64}{9}t^2\left(\frac{2t^2}{3}+1\right)\right]^{-1}\right),$$

shown in Fig. 7. It indicates positively decreasing behavior until $t = 2$ s, which then starts negatively deceasing for all values of t. This shows the violation of the SEC after $t = 2$ s representing accelerated expansion of the universe.

3.2. Nonvacuum case

In the nonvacuum case, action (4) includes the matter action S_M

$$S = \frac{1}{2\kappa^2}\int d^4x\sqrt{-g}[R + f(G)] + S_M.$$

We consider the dust fluid (fluid with zero pressure), for which the energy–momentum tensor is defined as

$$T_{\mu\nu} = \rho u_\mu u_\nu,$$

where ρ is the energy density and u_μ represents the 4-velocity. The conservation equation gives

$$\rho = \frac{\rho_0}{a^3}.$$

The Lagrangian takes the form

$$\mathcal{L} = -8\dot{a}^3\dot{G}f_{GG} + a^3[f(G) - Gf_G] + \rho_0,$$

yielding the same Euler–Lagrange equations as in the vacuum case, while the energy function becomes

$$\mathbb{E} = 24\frac{\dot{a}^3}{a^3} - \frac{1}{\dot{G}f_{GG}}(f(G) - Gf_G) - \rho_0.$$

The expressions for p^{eff} and ρ^{eff} are

$$p^{eff} = 16\frac{\dot{a}\ddot{a}}{a^3}\dot{G}f_G + 8\frac{\dot{a}^2}{a^2}\ddot{G}f_G + f(G) - Gf_G,$$

$$\rho^{eff} = 24\frac{\dot{a}^3}{a^3}\dot{G}f_{GG} - f(G) + Gf_G - \rho_0,$$

and the corresponding EoS parameter takes the form

$$\omega^{eff} = \frac{16\frac{\dot{a}\ddot{a}}{a^3}\dot{G}f_G + 8\frac{\dot{a}^2}{a^2}\ddot{G}f_G + f(G) - Gf_G}{24\frac{\dot{a}^3}{a^3}\dot{G}f_{GG} - f(G) + Gf_G - \rho_0}.$$

Figure 8 shows the behavior of the EoS parameter in the nonvacuum case for the model given in Eq. (28). The plot indicates a phantom-like DE era ($\omega^{eff} < -1$) and then asymptotically approaches -1 after $t = 4.5$ s. This shows the de Sitter fate of the universe as in the vacuum case.

4. CONCLUSIONS

Modified theories with their corresponding actions involving higher-order curvature as extra terms can lead to a better description of the phenomenon of cosmic accelerated expansion. In this context, we study solutions of the field equations in $f(G)$ (modified Gauss–Bonnet) gravity using the Noether symmetry approach for the FRW universe model by assuming vacuum and nonvacuum cases. In the nonvacuum case, we have taken dust fluid just for simplicity. The symmetry generators are found using separation of variables and a

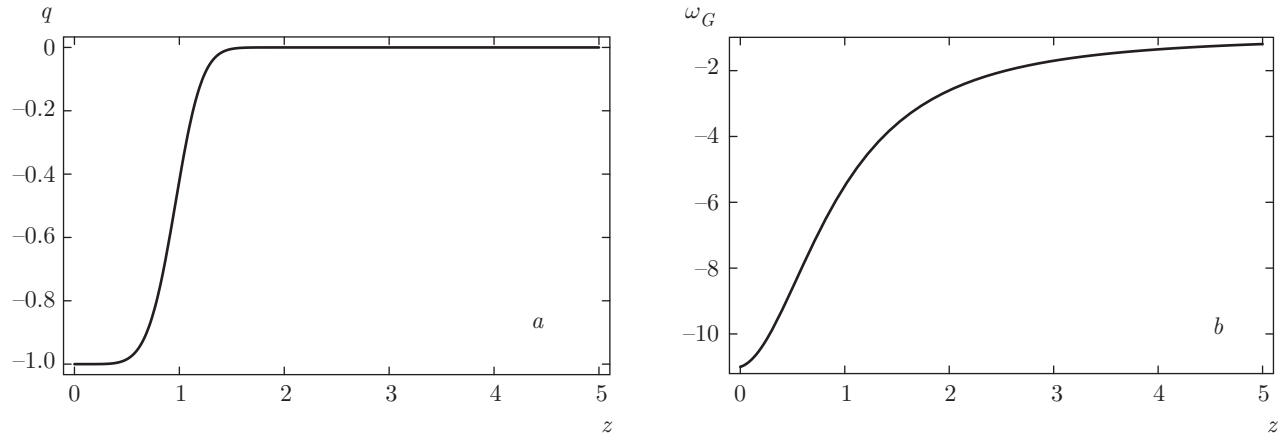

Fig. 4. Plots of the deceleration parameter q (a) and the EoS parameter ω_G (b) versus the redshift z

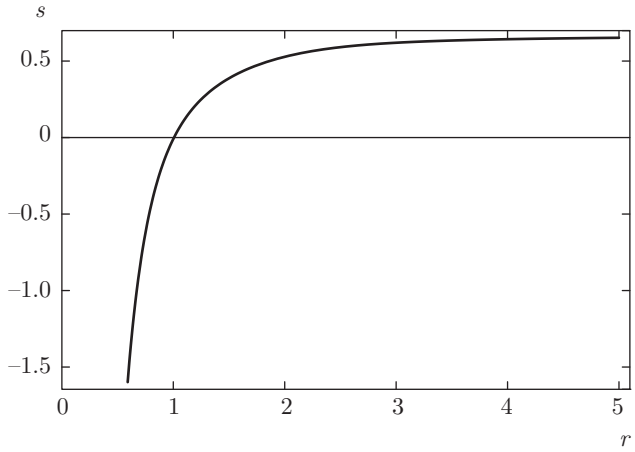

Fig. 5. Plot of the state-finder parameters (r, s)

power-law form. We have found the scale factor, the $f(G)$ model, and the corresponding conserved quantities. The deceleration and EoS parameters are also evaluated and used to discuss the expanding behavior of the universe. We have also explored the correspondence of the evaluated models with the ΛCDM model in terms of state-finder parameters.

The scale factor shows rapidly increasing behavior indicating the accelerating expansion of the universe. The negatively decreasing behavior of the deceleration parameter indicates cosmic expansion in the accelerating phase. The EoS parameters (separation of variables) crosses the phantom divide line to the phantom DE era and then approaches the de Sitter fate asymptotically, while it shows a phantom DE era and then approaches the de Sitter fate of the universe for the power-law form. We have checked the validity of energy conditions by assuming the WEC only in the vacuum case. The violation of the SEC indicates the accelerated expansion of the universe. It is well known that a positive energy density or pressure from matter or radiation can be added to any model satisfying the WEC; it still satisfies the WEC in the nonvacuum case. The EoS parameters for both methods in the vacuum case show almost the same behavior. These represent negative increasing behavior with increasing values of the redshift z, showing that the universe is in the present DE era, $\omega_G < -1$ (phantom-fluid-dominated era) in the far future. Their behavior in Fig. 2a and 4b shows that our constructed models are consistent with recent astrophysical observations [33, 34]. Also, Fig. 8 indicates that the EoS parameter remains close to the value -1, which shows the de Sitter fate of the universe in the nonvacuum case. The state-finder parameters indicate the correspondence of the resulting model with the ΛCDM model.

Sharif and Nawazish [29] have found exact solution for the LRS BI universe using the Noether symmetry approach with a power-law $f(R)$ model. The corresponding Hubble and deceleration parameters respectively become finite and negative versus time t. The EoS parameter showed crossing of the phantom dividing line from the quintessence to the phantom era. In [16], we have discussed energy conditions for the LRS BI model in $f(G)$ gravity with a perfect fluid. We took two specific $f(G)$ models with present-day values of the Hubble, deceleration, jerk, and snap parameters and found that the WEC and NEC are satisfied. The SEC is violated for both models, which represents the accelerated expansion of the universe. In this paper, we have found exact solutions for the FRW universe model in $f(G)$ gravity via Noether symmetry. Evolution of the universe has been discussed in terms of

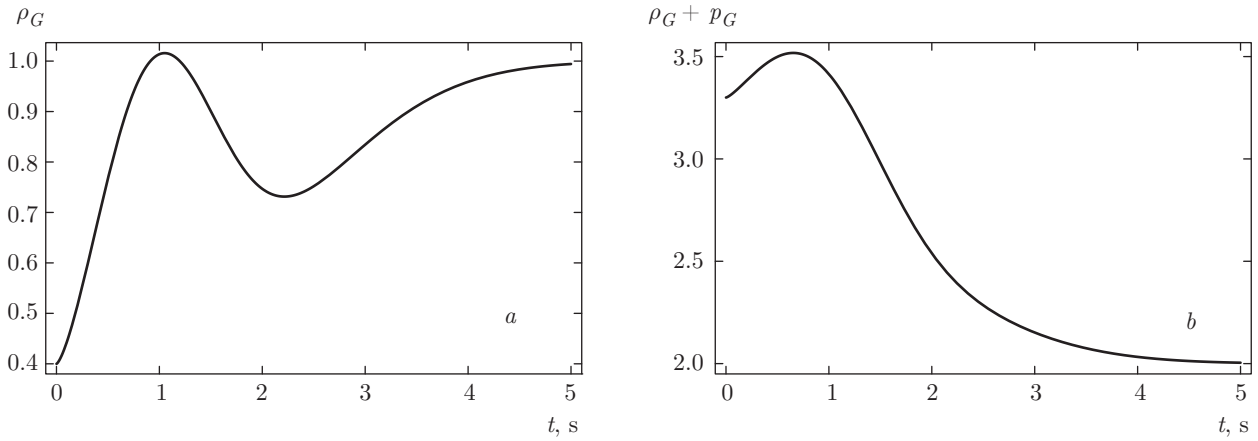

Fig. 6. Plots of the WEC versus t, (a) represents ρ_G and (b) represents $\rho_G + p_G$ versus t

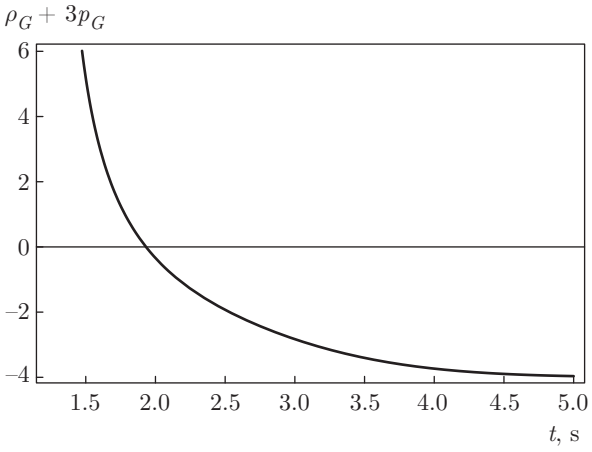

Fig. 7. Plots of the SEC ($\rho_G + 3p_G$) versus t

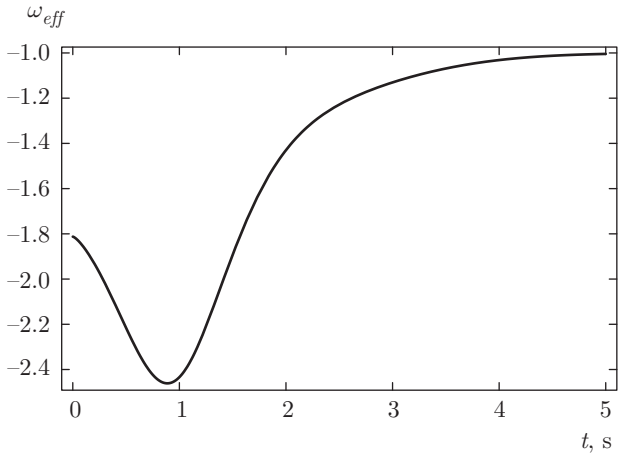

Fig. 8. Plot of the EoS parameter ω^{eff} versus time t in the nonvacuum case with $k_1 = 1$ and $\rho_0 = 1.5$

energy conditions, EoS, and deceleration parameters. The violation of the SEC and behavior of the deceleration parameter show an accelerating expansion of the universe. The state-finder parameters and negatively increasing behavior of the EoS parameter with the increasing values of the redshift show the consistency of our constructed models with recent cosmological observations.

REFERENCES

1. E. J. Copeland, M. Sami, and S. Tsujikawa, Int. J. Mod. Phys. D **15**, 1753 (2006).

2. R. Durrer and R. Maartens, Gen. Rel. Grav. **40**, 301 (2008).

3. M. C. Bento, O. Bertolami, and A. A. Sen, Phys. Rev. D **66**, 043507 (2002).

4. A. Sheykhi and M. Jamil, Phys. Lett. B **694**, 284 (2011).

5. K. Bamba, S. Capozziello, S. Nojiri, and S. D. Odintsov, Astrophys. Space Sci. **342**, 155 (2012).

6. S. Nojiri, S. D. Odintsov, and O. G. Gorbunova, J. Phys. A: Math. Gen. **39**, 6627 (2006).

7. G. Cognola et al., Astrophys. J. **664**, 687 (2007).

8. D. A. Easson, Int. J. Mod. Phys. A **19**, 5343 (2005).

9. S. Nojiri, S. D. Odintsov, and M. Sasaki, Phys. Rev. D **71**, 123509 (2005).

10. B. M. N. Carter and I. P. Neupane, J. Cosmol. Astropart. Phys. **06**, 004 (2006).

11. S. Nojiri, S. D. Odintsov, and S. Zerbini, Phys. Rev. D **75**, 086002 (2007).

12. H. M. Sadjadi, Phys. Scripta **83**, 055006 (2011).

13. S. Chatterjee and M. Parikh, Class. Quant. Grav. **31**, 155007 (2014).

14. M. Sharif and H. I. Fatima, Astrophys. Space Sci. **354**, 2124 (2014).

15. N. M. Garcia et al., Phys. Rev. D **83**, 104032 (2011).

16. M. Sharif and H. I. Fatima, Astrophys. Space Sci. **353**, 259 (2014).

17. J. Santos et al., Phys. Rev. D **76**, 083513 (2007).

18. M. Demianski et al., Phys. Rev. D **46**, 1391 (1992).

19. S. Capozziello and G. Lambiase, Gen. Rel. Grav. **32**, 673 (2000).

20. H. Wei, X. J. Guo, and L. F. Wang, Phys. Lett. B **707**, 298 (2012).

21. A. Paliathanasis et al., Phys. Rev. D **89**, 104042 (2014).

22. M. Sharif and S. Waheed, J. Cosmol. Astropart. Phys. **02**, 043 (2013).

23. B. Vakili, Phys. Lett. B **738**, 488 (2014).

24. M. Sharif and S. Waheed, Canad. J. Phys. **88**, 833 (2010).

25. M. F. Shamir, A. Jhangeer, and A. A. Bhatti, Chin. Phys. Lett. **29**, 080402 (2012).

26. M. Roshan and F. Shojai, Phys. Lett. B **668**, 238 (2008).

27. S. Capozziello, M. D. Laurentis, and S. D. Odintsov, Mod. Phys. Lett. A **29**, 1450164 (2014).

28. M. Sharif and I. Shafique, Phys. Rev. D **90**, 084033 (2014).

29. M. Sharif and I. Nawazish, J. Exp. Theor. Phys. **120**, 49 (2015).

30. I. Hussain and F. M. Mahomed, Canad. J. Phys. **90**, 467 (2012).

31. D. E. Neuenschwander, *Emmy Noether's Wonderful Theorem*, John's Hopkins Univ. Press, Baltimore (2011).

32. B. J. Li, D. B. John, and F. M. David, Phys. Rev. D **76**, 44027 (2007).

33. H. K. Jassal, J. S. Bagla, and T. Padmanabhan, Month. Not. Roy. Astron. Soc. **405**, 2639 (2010).

34. P. Wu and H. Yu, Europ. Phys. J. C **71**, 1552 (2011).